NANO LETTERS

Letter

pubs.acs.org/NanoLett

Nanocomposite Gold-Silk Nanofibers

Tzahi Cohen-Karni,[†,§] Kyung Jae Jeong,[†,§] Jonathan H. Tsui,[†,§] Gally Reznor,[§] Mirela Mustata,[⊥] Meni Wanunu,[⊥] Adam Graham,[#] Carolyn Marks,[#] David C. Bell,[#,∥] Robert Langer,[‡] and Daniel S. Kohane*[,§]

[†]David H. Koch Institute for Integrative Cancer Research and [‡]Department of Chemical Engineering, Massachusetts Institute of Technology (MIT), Cambridge, Massachusetts 02139, United States

[§]Laboratory for Biomaterials and Drug Delivery, Department of Anesthesiology, Division of Critical Care Medicine, Boston Children's Hospital, Harvard Medical School, 300 Longwood Avenue, Boston, Massachusetts 02115, United States

[⊥]Department of Physics, Dana Research Center, Northeastern University, Boston, Massachusetts 02115, United States

[∥]School of Engineering and Applied Science and [#]Center for Nanoscale Systems, Harvard University, Cambridge, Massachusetts 02138, United States

Supporting Information

ABSTRACT: Cell-biomaterial interactions can be controlled by modifying the surface chemistry or nanotopography of the material, to induce cell proliferation and differentiation if desired. Here we combine both approaches in forming silk nanofibers (SNFs) containing gold nanoparticles (AuNPs) and subsequently chemically modifying the fibers. Silk fibroin mixed with gold seed nanoparticles was electrospun to form SNFs doped with gold seed nanoparticles (SNF_{seed}). Following gold reduction, there was a 2-fold increase in particle diameter confirmed by the appearance of a strong absorption peak at 525 nm. AuNPs were dispersed throughout the AuNP-doped silk nanofibers ($SNFs_{Au}$). The Young's modulus of the $SNFs_{Au}$ was almost 70% higher than that of SNFs. $SNFs_{Au}$ were modified with the arginine-glycine-aspartic acid (RGD) peptide. Human mesenchymal stem cells that were cultured on RGD-modified SNF_{Au} had a more than 2-fold larger cell area compared to the cells cultured on bare SNFs; SNF_{Au} also increased cell size. This approach may be used to alter the cell−material interface in tissue engineering and other applications.

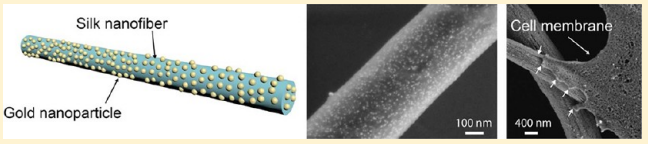

KEYWORDS: *Silk, nanofibers, gold nanoparticles, cellular adhesion, tissue engineering, mesenchymal stem cells*

A common challenge in engineering tissues is designing the structural biomaterials so as to mimic the natural microenvironment.[1] One approach to addressing this issue has been to modify the chemistry of the substrate on which cells would grow to enhance cell adhesion, proliferation, and differentiation. Such modification has been achieved with biological structural motifs, such as extracellular matrix proteins (e.g., fibronectin,[2] collagen, and elastin),[3] or with synthetic polymers or naturally occurring structural materials whose surface and chemical properties have been altered to impart biological functionality.[4] Another approach has been to alter the nanotopography of the substrate so as to influence cell behavior.

Studies of cell adhesion to surfaces have focused on two-dimensional (2D) geometries where surface ligands were immobilized in a controlled manner,[5] and their effect on cellular adhesion has been explored as a function of ligand island size and separation.[6] Application of these ideas in tissue engineering and other fields will necessitate their adaptation to three-dimensional (3D) nanostructured materials with well-defined surface chemistries, topographies, and mechanical properties.

Here, we combine these approaches by creating a 3D silk nanofiber matrix by electrospinning, incorporating gold nanoparticles (AuNPs) on and within the resulting fibers, and subsequently chemically modifying the AuNP surfaces to immobilize molecules on the nanofiber, specifically an integrin-binding cell adhesive peptide, arginine-glycine-aspartic acid motif (RGD).[7] The nanotopography imparted to the silk fibers by incorporation of gold particles was itself intended to

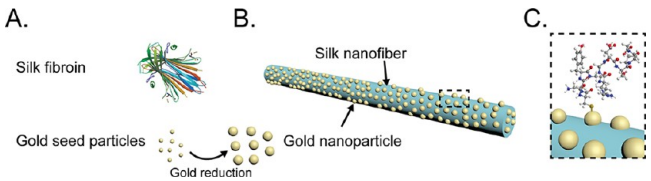

Figure 1. Synthesis and fabrication of AuNPs-doped SNF. (A) The building blocks: silk fibroin and gold seed nanoparticles. (B) A SNF doped with AuNPs (SNF_{Au}) on the surface and throughout the fiber cross section. (C) An illustration of surface modification of the SNF_{Au}. In this case the surface of the AuNPs was chemically modified with RGD motif peptide.

Received: July 29, 2012
Revised: August 27, 2012
Published: August 28, 2012

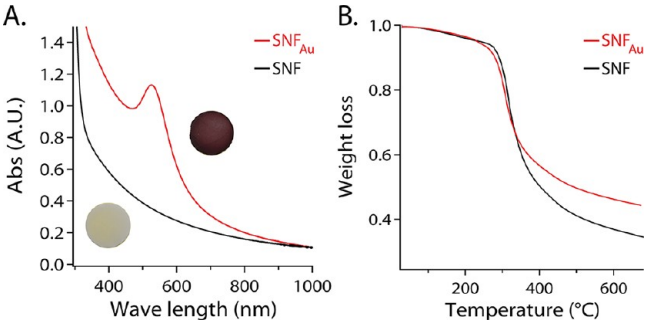

Figure 2. SNF characterization. (A) UV–vis optical properties of SNF and SNF_{Au}. (B) TGA of SNF and SNF_{Au}. Each trace is representative of four samples. Insets are images of mats of the respective materials.

enhance cell–material interactions: nanostructures and nanostructured surfaces have been shown to enhance cellular adhesion, proliferation, and differentiation.[8−10] We used silk as a model material because of its desirable mechanical properties, biocompatibility,[11] and possible uses as a scaffold in engineered tissue.[12] A straightforward method of altering the surface and chemical properties of silk to control the interface between cells and scaffold, as we provide here, has not been achieved to date.

Our approach to preparing AuNP-doped silk nanofibers (SNF_{Au}) is illustrated in Figure 1 (see also Materials and Methods in Supporting Information). Silk fibroin was extracted from *Bombyx mori* silkworm silk.[13] Silk fibroin solutions with or without gold seed nanoparticles[14] were electrospun[13] to form SNFs and SNFs containing seed particles (SNF_{seed}), respectively (Figure S1). SNFs doped with seed particles were reduced at room temperature in Au^+ solution for 3–4 days, producing SNFs with AuNPs on the surface and within the bulk of the material (SNF_{Au}) (Figure 1B). For cell adhesion studies, the fibers were modified with RGD peptide[15] (Figure 1C).

SNF_{Au} mats were maroon, while the SNF were white (Figure 2A insets). To quantify this observation, a UV–vis spectrum was acquired (Figure 2A). While the SNF had no characteristic absorption peaks on UV–vis spectroscopy, the SNF_{Au} had a strong absorption peak at 525 nm that is characteristic of AuNPs in the size range from 5 to 10 nm.[16] The UV–vis spectrum of SNF_{seed} did not show this absorption peak (Figure S2A). Moreover, the UV–vis spectrum of a SNF incubated in Au^+ solution for 6 days showed no absorption peaks, indicating that the gold seed nanoparticles are needed to form the AuNPs (Figure S2B). The gold contents of SNF_{Au} and SNF_{seed} as determined by thermogravimetric analysis (TGA) (Figure 2B and Figure S2C) were 10.4 ± 0.4% and 5.1 ± 0.1%, respectively; these results further confirmed our hypothesis that the gold content of the fibers increased due to the reduction of Au^+ ions at the surface of Au seeds during incubation.

SNF and SNF_{Au} were 428 ± 45 and 401 ± 58 nm in diameter, respectively (Figure 3; n = 30). The surface of the SNF (Figure 3A I,II) was relatively smooth, while the surface of the SNF_{Au} (Figure 3B I,II and Figure S3) was rough. Elemental mapping using energy dispersive spectroscopy (EDS) confirmed that the fibers contained gold (Figure S4). Cross-sectional transmission electron microscopy (TEM; Figure 3C) imaging showed that the gold was reduced and formed nanoparticles throughout the fiber diameter and length (Figure 3C). The resultant gold nanoparticles had an average diameter

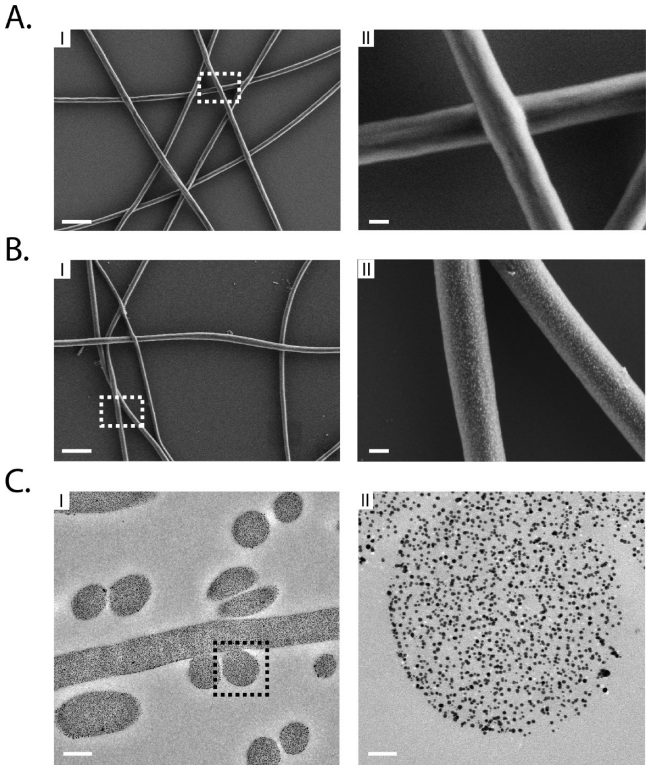

Figure 3. SNF surface and morphology. (A) I. SEM image of SNFs. Scale bar is 2.5 μm. II. Higher power view of the dashed white box. Scale bar is 200 nm. (B) I. SEM image of SNF_{Au}. Scale bar is 2.5 μm. II. Higher power view of the dashed white box. Scale bar is 200 nm. (C) I. Cross-sectional TEM image of SNF_{Au}. Scale bar is 400 nm. II. Higher power view of the dashed black box. Scale bar is 60 nm.

of 6.6 ± 1.0 nm (n = 479), a more than 2-fold increase in particle size compared to the original seed diameter of 3.2 ± 0.7 nm (n = 135) (Figure S1).

Recently it was demonstrated that incorporation of nanoparticles in silk thin films altered their mechanical properties,[17] specifically their Young's modulus. To investigate the effect of AuNPs on SNF mechanical properties, a single layer of fibers on a Si/600 nm SiO_2 substrate was prepared (see Materials and Methods, Supporting Information). The peak force quantitative nano mechanics scanning method (PFQNM)[18,19] (see Materials and Methods, Supporting Information) was used to map the elastic moduli of the SNF and SNF_{Au}. (Figure 4A I,II; see also Figure S5 for Z height plots of the same fibers). The average elastic modulus of SNF was 11.7 ± 2.3 GPa, which is consistent with the published mechanical properties of silk fibers.[20] The average elastic modulus of SNF_{Au} was 17.7 ± 2.1 GPa, almost 70% higher than that of SNF (Figure 4B and C). While we only used AuNPs, different materials could be loaded in silk in the same manner with potentially differing effects on mechanical properties. The ease of dispersion and homogeneity of nanoparticles throughout the material could allow the facile tailoring of material properties to specific applications.

Modification with AuNP could affect a wide range of cell behaviors by altering the nanotopography of the material. Furthermore, the AuNP enable straightforward chemical surface modifications that could further affect cell interaction. Preliminary to exploring the interaction between cells and the SNF-based substrates we studied the cytotoxicity of SNFs using PC12 cells, a cell line commonly used in toxicology; neither SNF_{seed} nor SNF_{Au} showed cytotoxicity for 96 h after initial

dx.doi.org/10.1021/nl302810c | *Nano Lett.* 2012, 12, 5403−5406

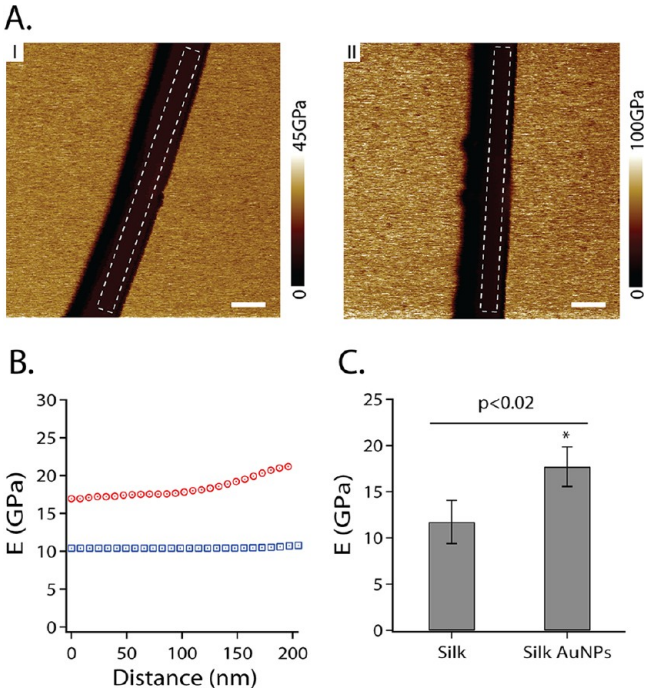

Figure 4. SNF mechanical properties. (A) I. Elastic modulus map of SNF. Scale bar is 250 nm. II. Elastic modulus map of SNF_{Au}. Scale bar is 250 nm. (B) Box cross-section curves of both SNF (blue open squares) and SNF_{Au} (red open circles), calculated from the elastic modulus (E) maps for the white dashed boxes. (C) Summary of the elastic modulus for both SNF and SNF_{Au}, the presented data are mean ± SD (n = 12).

exposure (see Materials and Methods and Figure S6, Supporting Information).

Adhesion of human mesenchymal stem cells (hMSCs) on SNF, SNF_{Au}, and either one after incubation with the integrin-binding peptide RGD (SNF + RGD and SNF_{Au} + RGD)[7,15] was observed 24 h after the initial seeding (see Materials and Methods, Supporting Information). The peptide readily forms covalent bonds to the AuNPs through the free thiol on cysteine residues,[21] whereas its binding to SNF is through weak physisorption to the fiber surface.[22] We measured the size of the individual cultured cells (termed individual cell area) and the number of cells per unit area of substrate (termed cell density). Both SNF_{Au} and SNF_{Au} + RGD showed a marked increase in cell size compared to both SNF and SNF + RGD (Figure 5A). In addition, SNF_{Au} + RGD showed an increase in cell density compared to both SNF and SNF + RGD (Figure 5B). These two findings indicate that cellular spreading was enhanced by surface nanostructure and, in combination with RGD, cell adhesion and/or proliferation, consistent with previous reports that RGD modification coupled with nanotopography enhances cell adhesion.[8,10,23,24]

The effects of the various SNF fiber types on the cytoskeletal development and cell morphology of hMSCs were examined. Well-developed cytoskeletal structures, as indicated by the presence and density of actin fibers, were observed in cells exposed to SNF_{Au} or SNF_{Au} + RGD (Figure 5C III,IV and Figure S7), whereas cells cultured on SNFs or SNF+RGD exhibited a faint signal of unstructured actin (Figure 5C I,II and Figure S7).

Nanostructured surfaces increase the formation of focal adhesions that eventually lead to a well-developed cytoskeleton.[25,26] There was a close interaction between the cell membrane and the AuNPs on SNF_{Au}, as can be seen in Figure 5D (I,II). The cells extended broad protrusions onto the fibers (Figure 5D II, marked with white arrows); such were not seen in unmodified SNPs, where only spare filamentous connections were seen (Figure S8). The broad protrusions seen in gold-containing fibers may correspond with focal interactions with AuNPs; this view is consistent with previous reports.[5,6,25,26]

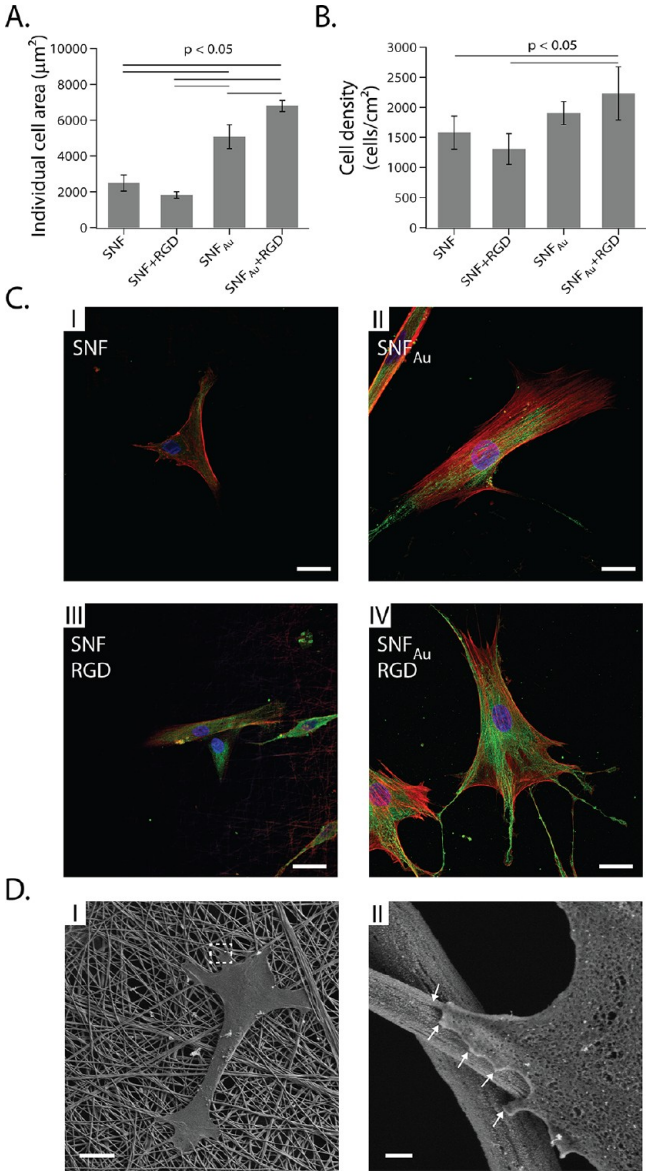

Figure 5. SNF cell interactions. (A) Area of individual hMSCs cultured on SNF, SNF_{Au}, SNF_{Au} + RGD, or SNF + RGD (n = 4). (B) Density of adhered hMSCs (Cell density) cultured on SNF, SNF_{Au}, SNF_{Au} + RGD, or SNF + RGD (n = 4). (For both panels A and B, data are mean ± SD). (C) Confocal imaging of (I) SNF, (II) SNF_{Au}, (III) SNF + RGD, and (IV) SNF_{Au} + RGD (II). Stains: nucleus (blue), actin filaments (red), and vinculin (green). Scale bar is 25 μm (D) I. Morphology of hMSC cultured on SNF_{Au} + RGD. Scale bar is 20 μm. II. Expanded view of the white dashed box, white arrow mark adhesion points. Scale bar is 400 nm.

We have demonstrated the synthesis of SNFs doped with AuNPs dispersed throughout the fiber cross-section (radially and longitudinally). The AuNPs have a strong absorption at 525 nm, an absorption wavelength that corresponds to AuNPs

dx.doi.org/10.1021/nl302810c | Nano Lett. 2012, 12, 5403−5406

as small as 5−10 nm in size. Doping with AuNPs improved the mechanical properties of silk significantly. The SNF_{Au} were not cytotoxic. The AuNPs coating the surface of the nanofibers were readily accessible for chemical surface modification. The SNF_{Au} showed an increase in the cell area and the number of adhered cells compared to bare SNFs (irrespective of modification with RGD).

This nanofiber preparation approach can be used to prepare fibers that are easily chemically modified to include chemical cues important to cellular proliferation and differentiation.[27,28] Moreover this platform allows a straightforward method to control cell microenvironment through a single-step chemical modification, with potential uses in tissue engineering. These materials could also be used as smart (e.g., light-triggered) or optically active substrates.

■ ASSOCIATED CONTENT

Supporting Information

Materials and Methods. Figures S1−S8. This material is available free of charge via the Internet at http://pubs.acs.org.

■ AUTHOR INFORMATION

Corresponding Author

*E-mail: Daniel.Kohane@childrens.harvard.edu

Notes

The authors declare no competing financial interest.

■ ACKNOWLEDGMENTS

T.C.-K. would like to thank the Juvenile Diabetes Research Foundation (JDRF), R.L. would like to acknowledge the Max Planck Award and funding from NIH grants R37-EB000244 and R01-EB006365, and D.S.K. would like to acknowledge funding from NIH grant GM073626.

■ REFERENCES

(1) Dvir, T.; Timko, B. P.; Kohane, D. S.; Langer, R. Nanotechnological strategies for engineering complex tissues. *Nat. Nanotechnol.* **2011**, *6* (1), 13−22.

(2) Feinberg, A. W.; Parker, K. K. Surface-Initiated Assembly of Protein Nanofabrics. *Nano Lett.* **2010**, *10* (6), 2184−2191.

(3) Hu, X.; Cebe, P.; Weiss, A. S.; Omenetto, F.; Kaplan, D. L. Protein-based composite materials. *Mater. Today* **2012**, *15* (5), 208−215.

(4) Tsur-Gang, O.; Ruvinov, E.; Landa, N.; Holbova, R.; Feinberg, M. S.; Leor, J.; Cohen, S. The effects of peptide-based modification of alginate on left ventricular remodeling and function after myocardial infarction. *Biomaterials* **2009**, *30* (2), 189−195.

(5) Graeter, S. V.; Huang, J. H.; Perschmann, N.; Lopez-Garcia, M.; Kessler, H.; Ding, J. D.; Spatz, J. P. Mimicking cellular environments by nanostructured soft interfaces. *Nano Lett* **2007**, *7* (5), 1413−1418.

(6) Cavalcanti-Adam, E. A.; Volberg, T.; Micoulet, A.; Kessler, H.; Geiger, B.; Spatz, J. P. Cell spreading and focal adhesion dynamics are regulated by spacing of integrin ligands. *Biophys. J.* **2007**, *92* (8), 2964−2974.

(7) Ruoslahti, E. RGD and other recognition sequences for integrins. *Annu. Rev. Cell Dev. Biol.* **1996**, *12*, 697−715.

(8) Stevens, M. M.; George, J. H. Exploring and engineering the cell surface interface. *Science* **2005**, *310* (5751), 1135−1138.

(9) Sniadecki, N.; Desai, R. A.; Ruiz, S. A.; Chen, C. S. Nanotechnology for cell-substrate interactions. *Ann. Biomed. Eng.* **2006**, *34* (1), 59−74.

(10) Park, J.; Bauer, S.; von der Mark, K.; Schmuki, P. Nanosize and vitality: TiO2 nanotube diameter directs cell fate. *Nano Lett.* **2007**, *7* (6), 1686−1691.

(11) Altman, G. H.; Diaz, F.; Jakuba, C.; Calabro, T.; Horan, R. L.; Chen, J. S.; Lu, H.; Richmond, J.; Kaplan, D. L. Silk-based biomaterials. *Biomaterials* **2003**, *24* (3), 401−416.

(12) Zhang, X. H.; Reagan, M. R.; Kaplan, D. L. Electrospun silk biomaterial scaffolds for regenerative medicine. *Adv. Drug Delivery Rev.* **2009**, *61* (12), 988−1006.

(13) Rockwood, D. N.; Preda, R. C.; Yucel, T.; Wang, X. Q.; Lovett, M. L.; Kaplan, D. L. Materials fabrication from Bombyx mori silk fibroin. *Nat. Protoc.* **2011**, *6* (10), 1612−1631.

(14) Duff, D. G.; Baiker, A.; Edwards, P. P. A new hydrosol of gold clusters 0.1. Formation and particle size variation. *Langmuir* **1993**, *9* (9), 2301−2309.

(15) VandeVondele, S.; Voros, J.; Hubbell, J. A. RGD-Grafted poly-l-lysine-graft-(polyethylene glycol) copolymers block non-specific protein adsorption while promoting cell adhesion. *Biotechnol. Bioeng.* **2003**, *82* (7), 784−790.

(16) Link, S.; El-Sayed, M. A. Size and temperature dependence of the plasmon absorption of colloidal gold nanoparticles. *J. Phys. Chem. B* **1999**, *103* (21), 4212−4217.

(17) Kharlampieva, E.; Kozlovskaya, V.; Gunawidjaja, R.; Shevchenko, V. V.; Vaia, R.; Naik, R. R.; Kaplan, D. L.; Tsukruk, V. V. Flexible Silk-Inorganic Nanocomposites: From Transparent to Highly Reflective. *Adv. Funct. Mater.* **2010**, *20* (5), 840−846.

(18) Adamcik, J.; Berquand, A.; Mezzenga, R. Single-step direct measurement of amyloid fibrils stiffness by peak force quantitative nanomechanical atomic force microscopy. *Appl. Phys. Lett.* **2011**, *98*, 19.

(19) Schon, P.; Bagdi, K.; Molnar, K.; Markus, P.; Pukanszky, B.; Vancso, G. J. Quantitative mapping of elastic moduli at the nanoscale in phase separated polyurethanes by AFM. *Eur. Polym. J.* **2011**, *47* (4), 692−698.

(20) Wang, M.; Jin, H. J.; Kaplan, D. L.; Rutledge, G. C. Mechanical properties of electrospun silk fibers. *Macromolecules* **2004**, *37* (18), 6856−6864.

(21) Levy, R.; Thanh, N. T. K.; Doty, R. C.; Hussain, I.; Nichols, R. J.; Schiffrin, D. J.; Brust, M.; Fernig, D. G. Rational and combinatorial design of peptide capping Ligands for gold nanoparticles. *J. Am. Chem. Soc.* **2004**, *126* (32), 10076−10084.

(22) Chen, J. S.; Altman, G. H.; Karageorgiou, V.; Horan, R.; Collette, A.; Volloch, V.; Colabro, T.; Kaplan, D. L. Human bone marrow stromal cell and ligament fibroblast responses on RGD-modified silk fibers. *J. Biomed. Mater. Res., Part A* **2003**, *67A* (2), 559−570.

(23) Lim, J. Y.; Donahue, H. J. Cell sensing and response to micro- and nanostructured surfaces produced by chemical and topographic patterning. *Tissue Eng.* **2007**, *13* (8), 1879−1891.

(24) Patla, I.; Volberg, T.; Elad, N.; Hirschfeld-Warneken, V.; Grashoff, C.; Fassler, R.; Spatz, J. P.; Geiger, B.; Medalia, O. Dissecting the molecular architecture of integrin adhesion sites by cryo-electron tomography. *Nat. Cell Biol.* **2010**, *12* (9), 909−915.

(25) Arnold, M.; Cavalcanti-Adam, E. A.; Glass, R.; Blummel, J.; Eck, W.; Kantlehner, M.; Kessler, H.; Spatz, J. P. Activation of integrin function by nanopatterned adhesive interfaces. *ChemPhysChem* **2004**, *5* (3), 383−388.

(26) Arnold, M.; Schwieder, M.; Blummel, J.; Cavalcanti-Adam, E. A.; Lopez-Garcia, M.; Kessler, H.; Geiger, B.; Spatz, J. P. Cell interactions with hierarchically structured nano-patterned adhesive surfaces. *Soft Matter* **2009**, *5* (1), 72−77.

(27) Guilak, F.; Cohen, D. M.; Estes, B. T.; Gimble, J. M.; Liedtke, W.; Chen, C. S. Control of Stem Cell Fate by Physical Interactions with the Extracellular Matrix. *Cell Stem Cell* **2009**, *5* (1), 17−26.

(28) Park, J.; Bauer, S.; Pittrof, A.; Killian, M. S.; Schmuki, P.; von der Mark, K. Synergistic Control of Mesenchymal Stem Cell Differentiation by Nanoscale Surface Geometry and Immobilized Growth Factors on TiO2 Nanotubes. *Small* **2012**, *8* (1), 98−107.